

# Cytoplasmic Regulation of the Movement of E-Cadherin on the Free Cell Surface as Studied by Optical Tweezers and Single Particle Tracking: Corraling and Tethering by the Membrane Skeleton

Yasushi Sako,\* Akira Nagafuchi,‡ Shoichiro Tsukita,‡ Masatoshi Takeichi,§ and Akihiro Kusumi\*

\*Department of Biological Science, Graduate School of Science, Nagoya University, Chikusa-ku, Nagoya 464-8602, Japan;

‡Department of Medical Chemistry, Faculty of Medicine, and §Department of Biophysics, Graduate School of Science, Kyoto University, Sakyo-ku, Kyoto 606-8502, Japan

**Abstract.** The translational movement of E-cadherin, a calcium-dependent cell–cell adhesion molecule in the plasma membrane in epithelial cells, and the mechanism of its regulation were studied using single particle tracking (SPT) and optical tweezers (OT). The wild type (Wild) and three types of artificial cytoplasmic mutants of E-cadherin were expressed in L-cells, and their movements were compared. Two mutants were E-cadherins that had deletions in the COOH terminus and lost the catenin-binding site(s) in the COOH terminus, with remaining 116 and 21 amino acids in the cytoplasmic domain (versus 152 amino acids for Wild); these are called Catenin-minus and Short-tailed in this paper, respectively. The third mutant, called Fusion, is a fusion protein between E-cadherin without the catenin-binding site and  $\alpha$ -catenin without its NH<sub>2</sub>-terminal half. These cadherins were labeled with 40-nm  $\phi$  colloidal gold or 210-nm  $\phi$  latex particles via a monoclonal antibody to the extracellular domain of E-cadherin for SPT or OT experiments, respectively. E-cadherin on the dorsal cell surface (outside the cell–cell contact region) was investigated. Catenin-minus and Short-tailed could be dragged an average of 1.1 and 1.8  $\mu$ m by OT

(trapping force of 0.8 pN), and exhibited average microscopic diffusion coefficients ( $D_{\text{micro}}$ ) of  $1.2 \times 10^{-10}$  and  $2.1 \times 10^{-10}$  cm<sup>2</sup>/s, respectively. Approximately 40% of Wild, Catenin-minus, and Short-tailed exhibited confined-type diffusion. The confinement area was 0.13  $\mu$ m<sup>2</sup> for Wild and Catenin-minus, while that for Short-tailed was greater by a factor of four. In contrast, Fusion could be dragged an average of only 140 nm by OT. Average  $D_{\text{micro}}$  for Fusion measured by SPT was small ( $0.2 \times 10^{-10}$  cm<sup>2</sup>/s). These results suggest that Fusion was bound to the cytoskeleton. Wild consists of two populations; about half behaves like Catenin-minus, and the other half behaves like Fusion. It is concluded that the movements of the wild-type E-cadherin in the plasma membrane are regulated via the cytoplasmic domain by (a) tethering to actin filaments through catenin(s) (like Fusion) and (b) a corraling effect of the network of the membrane skeleton (like Catenin-minus). The effective spring constants of the membrane skeleton that contribute to the tethering and corraling effects as measured by the dragging experiments were 30 and 5 pN/ $\mu$ m, respectively, indicating a difference in the skeletal structures that produce these two effects.

**E**-CADHERIN is a calcium-dependent cell-to-cell recognition/adhesion molecule in epithelial tissues, and a transmembrane protein that spans the plasma membrane once (Takeichi, 1988, 1991). E-cadherin is localized in cell-to-cell adherens junctions and is also found

in dilute homogeneous distributions over the free surface of cells (Bacallao et al., 1989). Cadherin molecules on the free cell surface may be surveying new physical contacts with other cells or may be on their way to the assembly of adherens junctions.

Some cytoplasmic proteins, including  $\alpha$ - and  $\beta$ -catenins and p120, are bound to the cytoplasmic domain of E-cadherin (Ozawa et al., 1989; McCrea et al., 1991; Reynolds and McCrea, 1994).  $\alpha$ -Catenin is an F-actin binding protein (Rimm et al., 1995). Binding of E-cadherin to actin through  $\alpha$ -catenin is essential for cadherin-mediated cell adhesion (Hirano et al., 1992; Nagafuchi et al., 1994; Watabe

Address all correspondence to Akihiro Kusumi, Department of Biological Science, Graduate School of Science, Nagoya University, Chikusa-ku, Nagoya 464-8602, Japan. Tel.: 011-81-52-789-2969. Fax: 011-81-52-789-2968. E-mail: akusumi@bio.nagoya-u.ac.jp

Y. Sako's present address is First Department of Physiology, Medical School of Osaka University, Yamadaoka, Suita, Osaka 565-0871, Japan.

et al., 1994). p120 is a  $\beta$ -catenin-, plakoglobin-related protein which makes a complex with E-cadherin and  $\alpha$ -catenin (Peifer et al., 1994; Jou et al., 1995; Shibamoto et al., 1995).

The association of newly synthesized  $\alpha$ -catenin with the cadherin-catenin complex takes place at the plasma membrane (Hinck et al., 1994). However, it is not known if all cadherin molecules are bound to the actin cytoskeleton, in addition, the stage of their assembly into adherens junctions at which they start being associated with actin filaments is also unclear. Furthermore, little knowledge is available regarding the mechanical properties of the actin filaments that are associated with cadherin molecules, although such information is necessary for understanding the mechanical basis of cadherin-based cell-cell adhesion.

Recently, we have demonstrated the existence of two major types of interactions between membrane-spanning proteins and the membrane-associated portion of the cytoskeleton (membrane skeleton) (Sako and Kusumi, 1994, 1995). The first type of interaction is binding to the membrane skeleton (Fig. 1 A, *Tether model*). The second type of interaction is that where membrane proteins are confined in compartments bounded by the network of the membrane skeleton (Fig. 1 B, *Fence model*). In this model, membrane proteins are not tethered to the membrane skeleton and are free to undergo Brownian diffusion, but are corralled in the membrane skeleton meshes because of the steric hindrance of the cytoplasmic domain of membrane proteins and the membrane skeleton. The movements of membrane proteins, including transferrin receptor and  $\alpha_2$ -macroglobulin receptor in a fibroblast (Sako and Kusumi, 1994, 1995), E-cadherin, transferrin receptor, and EGF receptor in a keratinocyte (Kusumi et al., 1993), and band 3 in erythrocyte (Sheetz et al., 1980; Tsuji and Ohnishi, 1986; Tsuji et al., 1988), can be explained using these two models.

These two models are based on findings obtained using single particle tracking (SPT)<sup>1</sup> (De Brabander et al., 1985; Gelles et al., 1988; Kucik et al., 1989) and optical tweezers (OT) (Ashkin et al., 1986, 1987). For example, in the plasma membrane of normal rat kidney (NRK) fibroblast cells, movements of 80–90% of the particles bound to the transferrin receptor were temporarily confined within compartments with an average diagonal length of 600 nm. Lateral diffusion over the cell surface takes place as a result of consecutive hops from one compartment to an adjacent compartment, which occurs an average of once every 20–30 s (intercompartmental hop diffusion). This population exhibited microscopic diffusion coefficients within compartments ( $D_{\text{micro}} > 1.5 \times 10^{-10} \text{ cm}^2/\text{s}$ ), suggesting free diffusion within a compartment. Such molecules could be dragged freely by OT until they hit the membrane skeleton fence. With a trapping force of 0.1 pN, half of this population escaped from OT at the boundaries of the membrane compartment. The remaining transferrin receptors (10–20%) exhibited  $D_{\text{micro}} < 1.5 \times 10^{-10} \text{ cm}^2/\text{s}$  and could not be dragged much even under a trapping force of 0.8 pN. It was concluded that these molecules are tethered to

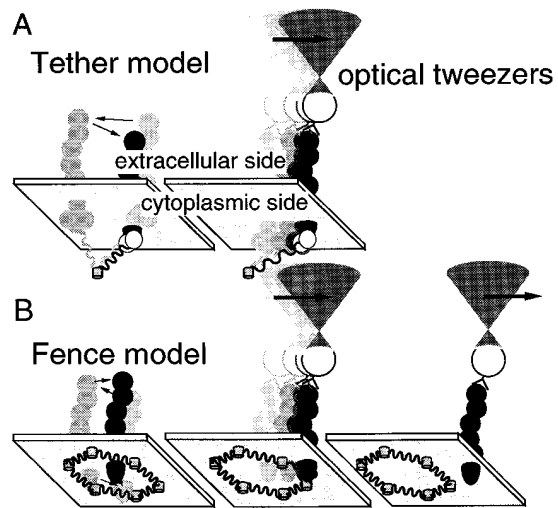


**Figure 1.** A tether model (A) and a fence model (B) proposed as mechanisms for the regulation of lateral movements of E-cadherin (Sako and Kusumi, 1995). These models are shown together with the optical tweezers experiments which may make it possible to differentiate and characterize these two mechanisms. (A) E-cadherin tethered to a cytoskeletal filament can be dragged only the length the filament is stretched, with a force of  $\approx 1$  pN or less. (B) An E-cadherin molecule free from tethering may be temporarily trapped within a compartment enclosed by the membrane skeleton fence. The particle-protein complex can pass across the fence if the dragging force by OT is high enough. For transferrin receptor in the plasma membrane of NRK cells, the force needed to pass across the fence is 0.05–0.1 pN (Sako and Kusumi, 1995).

the membrane undercoat structures or the membrane skeleton (Sako and Kusumi, 1994, 1995).

In the present study, we again used SPT and OT and studied the mechanisms of the regulation of the movements of the wild type and three artificial cytoplasmic mutants of E-cadherin. These molecules were artificially expressed in mouse L cells, in which the expression of intrinsic cadherin is not detectable.

The structures of the E-cadherins studied in this work are shown in Fig. 2. The wild-type E-cadherin (EL $\beta$  1a, Nose et al., 1988, called “Wild” in this paper) has a cytoplasmic domain of 152 amino acids (aa) at the COOH terminus. It includes a binding domain for  $\alpha$ - and  $\beta$ -catenins in the region 7–72 aa from the COOH terminus (Nagafuchi and Takeichi, 1989; Ozawa et al., 1990). Two mutants (EL $\beta$  21 and EL $\beta$  24; Nagafuchi and Takeichi, 1988) have deletions of 36 and 131 aa at the COOH terminus, leaving 116 and 21 aa in the cytoplasmic domain, respectively. These molecules lack a catenin-binding site(s), and are called “Catenin-minus” and “Short-tailed” in this paper, respectively. They cannot mediate cell-cell adhesion. One mutant (nE $\alpha$ CL1, called “Fusion” in this paper (Nagafuchi et al., 1994) is a fusion molecule of the COOH-terminal half (aa 508–906) of  $\alpha$ -catenin and E-cadherin that lost 72 aa in the COOH terminus. Fusion does not bind to either  $\alpha$ - or  $\beta$ -catenin. However, fusion can mediate cell-cell adhesion, probably because of the presence within the molecule of a part of  $\alpha$ -catenin that is capable of binding

1. *Abbreviations used in this paper:* MSD, square displacement averaged over a single particle's trajectory (running average over a single trajectory); OT, optical tweezers; SPT, single particle tracking.

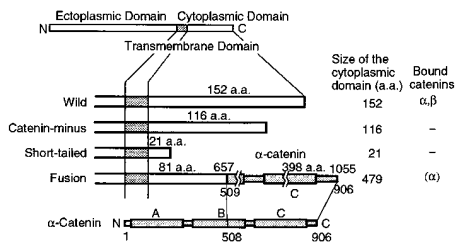


**Figure 2.** Structures of the wild-type E-cadherin and its artificial mutants used in this study. E-cadherin has a single transmembrane domain. Binding site(s) for catenins exists in the sequence of 7–72 aa from the COOH terminus (Nagafuchi and Takeichi, 1989; Ozawa et al., 1990). Wild type (*Wild*) contains 152 aa in the cytoplasmic domain. *Catenin-minus* and *Short-tailed* have deletions of 36 and 131 aa from the COOH terminus, leaving 116 and 21 aa, respectively, in the cytoplasmic domain. These molecules have lost binding sites for catenin(s). *Fusion* is a fusion protein of E-cadherin that lacks 72 aa at the COOH terminus fused with the COOH-terminal 508–906 aa of  $\alpha$ -catenin. Fusion does not have a catenin binding site. Rectangles (A, B, and C) in the molecular structures of  $\alpha$ -catenin and Fusion indicate regions homologous to vinculin (A, talin binding domain; B, function unknown; C, paxillin/vinculin binding domain (Nagafuchi et al., 1991).

to actin filaments (Nagafuchi et al., 1994). The structures of these cadherin molecules differ only in the cytoplasmic domain. The ectoplasmic and transmembrane domains are the same. The cytoplasmic domain is expected to affect the mobility of these molecules through (a) binding (ability or inability) to catenins and (b) the size (steric effect) of the cytoplasmic domain. Binding to catenin(s) would lead to tethering of cadherins to actin filaments near the cytoplasmic surface of the plasma membrane (see Fig. 1 A). The size of the cytoplasmic domain would affect the probability for the molecules to hop over the fence of the membrane skeleton network into an adjacent compartment (see Fig. 1 B).

In addition to observing the movements, E-cadherin on the free cell surface was dragged laterally along the plasma membrane by OT. By observing the response of E-cadherin to this dragging force, E-cadherin molecules that are either bound to or corralled in the membrane skeleton can be distinguished, and the mechanical properties of the membrane skeleton that regulate the movements of E-cadherin can be analyzed. We found that the mobility of Fusion was restricted by tethering to actin filaments through its  $\alpha$ -catenin portion, whereas the movements of Catenin-minus and Short-tailed were mainly regulated by the corraling effect of the membrane skeleton network. Half of Wild were tethered to, and the other half were confined by, the membrane skeleton. Both tethering and corraling structures were found to be elastic.

## Materials and Methods

### Cells

Mouse L-cells expressing Wild and mutant molecules after transfection and cloning were grown in MEM supplemented with 10% FCS. Cells cultured on a cover slip for 2 d after plating were used for the experiments. Cells transfected with cDNAs of Wild and Fusion showed cell–cell adhesion activity and, under optimal conditions, exhibited a cobblestone mor-

phology typical of epithelial cells, whereas cells transfected with cDNAs of Catenin-minus and Short-tailed did not.

### Preparation of Colloidal Gold and Latex Particles Coated with Anti-E-Cadherin mAb

Colloidal gold particles of 40 nm in diameter coated with anti-E-cadherin mAb (ECCD-2; Shirayoshi et al., 1986) were prepared as described previously (G40; Kusumi et al., 1993). Gold particles were incubated with ECCD-2 IgG at a ratio of 500 IgG molecules/particle. This is the minimal protecting amount (the lowest concentration of a protein concentration in a solution that is used to pretreat the gold particles necessary to stabilize the gold particles in suspension and avoid aggregation and sedimentation of gold particles) of IgG. To test the effect of multiple binding of E-cadherins to gold particles, gold particles coated with smaller amounts of E-cadherin specific Fab were prepared. In this case, gold particles were incubated with ECCD-2 Fab at a ratio of 100 Fab molecules/particle. This is about 1/10 the molar amount of the minimal protecting amount of Fab.

Latex particles coated with ECCD-2 were prepared in the following way. ECCD-2 (300  $\mu$ g) in 840  $\mu$ l PBS (150 mM NaCl, 10 mM sodium phosphate, pH 7.2) was centrifuged at 12,000 g for 10 min. The supernatant was mixed with 60  $\mu$ l of a suspension (2% solid) of 210-nm-diam latex particles (Polysciences Inc., Warrington, PA), vortexed for 10 s, and then incubated for 3 h at room temperature. BSA (10% in water, pH 7.0) was added as a stabilizer to a final concentration of 1%. After incubating for 1 h at room temperature, 5 ml PBS was added and the mixture was centrifuged at 12,000 g for 30 min. The precipitate was resuspended in 6 ml PBS by brief sonication and washed by two additional runs of centrifugation. After the final centrifugation, the precipitate was resuspended in 1 ml of HBSS buffered with Pipes, pH 7.2, containing 1% BSA (HBSS-BSA) by sonication, filtered through a 0.45- $\mu$ m filter (Millipore Corp., Bedford, MA), and then stored at 4°C (L210).

### Optical Trapping and Single Particle Tracking

Cells on a cover slip were incubated with 80  $\mu$ l of G40 or L210 suspension for 30 min at room temperature, washed three times with HBSS-BSA, and then mounted in MEM (less  $\text{NaHCO}_3$ ) containing 10% FCS buffered with 5 mM Pipes, pH 7.2, on a slide glass with spacers of 0.2-mm-thick adhesive tape. The particles to be dragged or observed were selected randomly from over the entire cell surface, except for regions of cell–cell contact.

The optical trapping apparatus was the same as that used by Sako and Kusumi (1995). Complexes of L210 and E-cadherin were captured with the focused beam of an Nd:YAG laser ( $\lambda = 1,064$  nm) and dragged laterally along the plasma membrane by moving the laser beam.

The maximal trapping force was 0.8 pN, and the dragging velocity was 0.6  $\mu$ m/s. SPT was carried out as described previously (Kusumi et al., 1993; Sako and Kusumi, 1994, 1995) using video-enhanced Nomarski microscopy. All experiments were performed at 37°C.

Movements of G40 and L210 particles on the cell surface were recorded on a laser disk video recorder (TQ3100-F; Panasonic, Osaka, Japan). Video sequences were digitized frame by frame with an image processor (DVS-3000; Hamamatsu Photonics, Hamamatsu, Japan) and (x, y) coordinates of particles in each video frame were calculated by a personal computer using the method described by Gelles et al. (1988). Usually, movements during 16.7 s (500 video frames) were recorded for SPT with G40.

### Data Analysis

Data analysis was basically the same as described previously (Kusumi et al., 1993; Sako and Kusumi, 1994, 1995). The mean square displacement (MSD) that is averaged over a trajectory at each time interval ( $\Delta t$ ) was calculated from the trajectory of a particle.  $D_{\text{micro}}$  was calculated as the slope of the MSD- $\Delta t$  plot for 67–133 ms (2–4 video frames, the displacement between time 0 and 67 ms was not included to avoid high frequency noise) by least-square fitting.

To determine the motional mode for each trajectory, MSD between 0 and 5 s ( $\text{MSD}_5$ ) was used (Kusumi et al., 1993). The method is briefly described below. Consider particles undergoing simple Brownian diffusion at an average rate of  $D_{\text{micro}}$ .  $\text{MSD}_5$  for simple Brownian particles after ensemble averaging over all of the particles will be  $4 \times D_{\text{micro}} \times 5$  s. If  $\text{MSD}_5$  for a test particle is significantly greater than or less than  $4 \times D_{\text{micro}} \times 5$  s, the probability that the particle is not undergoing simple diffusion increases; it may be undergoing directed movement or confined diffusion, respectively. Therefore, we introduce a convenient parameter to charac-

terize a trajectory of a test particle in terms of its deviation in MSD from the ensemble averaged MSD expected for simple Brownian particles possessing the same  $D_{\text{micro}}$  as the test particle, i.e., RD (for relative deviation) =  $\text{MSD}_5/(4 \times D_{\text{micro}} \times 5 \text{ s})$  (Kusumi et al., 1993). Since diffusion is a stochastic process, we generated 2,000 simple Brownian trajectories in a computer and obtained the distribution of the ratio  $\text{MSD}_5/(4 \times D_{\text{micro}} \times 5 \text{ s})$  (=  $\text{RD}_{\text{sim}}$ ). For each experimental trajectory, we calculated  $\text{MSD}_5/(4 \times D_{\text{micro}} \times 5 \text{ s})$  (=  $\text{RD}_{\text{exp}}$ ), and determined whether this value was within 2.5% from either end of the distribution of  $\text{RD}_{\text{sim}}$ . When  $\text{RD}_{\text{exp}}$  was within the middle 95% of the distribution of  $\text{RD}_{\text{sim}}$ , the trajectory was classified as simple Brownian diffusion. When  $\text{RD}_{\text{exp}}$  was within 2.5% from the high (low) end of the distribution of  $\text{RD}_{\text{sim}}$ , the trajectory was classified as directed (confined) diffusion.

The size of the confinement area and the drift velocity of directed movement were estimated by fitting the  $\text{MSD}-\Delta t$  plot from  $\Delta t = 0-5 \text{ s}$  using equations we derived previously (Kusumi et al., 1993).

## Results

### Specificity and Multiplicity of Binding

E-cadherin molecules on the living cell surface were labeled with 40-nm  $\phi$  colloidal gold particles or 210-nm  $\phi$  latex particles coated with anti-E-cadherin monoclonal antibody (G40 or L210, respectively). An average of 20 G40 or L210 particles per cell were bound to the cell surface. The number of particles bound to the cells vary from one cell to another (10–40 particles per cell), and its variations for different cell types were smaller than cell-to-cell variations. Difference in the type of particles, i.e., gold and latex particles, made no difference in terms of the number of particles bound to the cell surface for all cell types used in the present work (similar ranges and averages as above). Particles coated only with BSA, without antibody IgG or Fab, were not bound to cells (only at a level of a few particles per cell for all types of cells used in the present work). These results suggest high binding specificities of these probes. Previously, we have shown that incubation of keratinocytes expressing higher levels of E-cadherin with the particles in the presence of a 100-fold excess amount of free ECCD-2 IgG (which was premixed with the particles before addition to cells) reduced the binding of these particles to only several particles/cell. This result again indicates that the binding is specific for E-cadherin.

This result also suggests that the avidity effect, i.e., the increases in the effective binding rate and/or the effective binding constant of ECCD-2 IgG because of multivalency of the particles, was small. In the present investigation, G40 coated with antibody Fab at molar concentrations 5–10 times less than those for antibody IgG (G40-Fab and G40-IgG, respectively) were bound to the cell surface equally well as particles coated with antibody IgG at higher concentrations. As described above, both gold and latex particles were bound to the cell surface at a similar level. Taken together, these results suggest that these particles were bound to a single or a small group of E-cadherin molecules. Difference in motional characteristics of G40-IgG and G40-Fab (and also L210-IgG) is described later in the present report (virtually no difference). Mecham et al. (1991) also suggested that the gold particles behave as individual ligand molecules and can be used to predict both the location and binding properties when they studied the elastin/laminin binding protein using single particle tracking.

The level of cross-linking by the particle probes would also depend on the concentration of cadherin on the cell

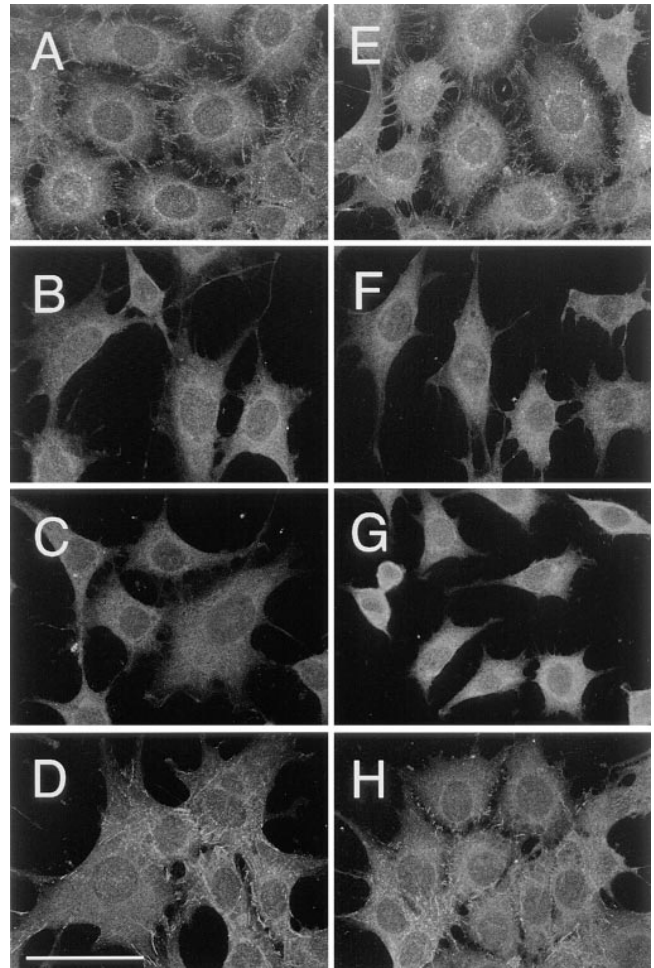


**Figure 3.** Indirect immunofluorescence staining of E-cadherin on the surface of cells transfected with E-cadherin cDNAs. Cells before (A–D) and after (E–H) incubation with ECCD-2-G40 were fixed with cold methanol, and E-cadherin on the cell surface was stained with ECCD-2 and FITC-labeled anti-rat IgG. Images were obtained by a confocal laser scanning microscopy, with a focal plane at about the height of the dorsal free cell surface near the peripheries of the cell. Staining on the plasma membrane over the nucleus was not observed because it is out of focus. A and E, Wild; B and F, Catenin-minus; C and G, Short-tailed; and D and H, Fusion. Bar, 50  $\mu\text{m}$ .

surface (expression levels) and local concentration or intrinsic aggregation of cadherin. Another possibility is that induction of small aggregation by gold particles causes formation of large aggregates around the particle-induced aggregates. To examine such possibilities, E-cadherins were stained by indirect immunofluorescence, and the stained cells were observed by confocal laser scanning fluorescence microscopy (Fig. 3, the focus is set at about the height of the free cell surface near peripheries of the cell). Amounts of various cadherins expressed in cells look similar to each other (Fig. 3, A–D). Small aggregates outside the region of cell–cell contact may exist, but the amounts of aggregates are similar for different cadherins (larger punctates seen in wild-type cells are localized intracellularly, perhaps representing intracellular pools). Addition of G40 did not change the staining patterns (Fig. 3, E–H).

The tendency that Fusion becomes aggregated after addition of the particle probes on the cell surface is not more than the tendencies of others. In addition, the extracellular domain is the same for all types of E-cadherin molecules. Therefore, it is not very likely that one type of cadherin mutants used in this work stuck to the particles more than others.

### Lateral Dragging of Particle–E-Cadherin Complexes

A single-beam gradient optical trap (Ashkin et al., 1986, 1987) was used to capture and drag L210–E-cadherin complexes laterally along the plasma membrane. The maximal trapping force was 0.8 pN and the optical trap was moved at a velocity of 0.6  $\mu\text{m/s}$  (Sako and Kusumi, 1995) for up to 5  $\mu\text{m}$ . The direction of dragging was chosen randomly. Since we are interested in the mechanisms that regulate the movements and assembly process of E-cadherin, particles outside the region of cell–cell contact were selected for the dragging experiments. Particles bound to E-cadherin at sites of cell–cell contact exhibited small movements (Kusumi et al., 1993). Complexes of 40-nm  $\phi$  colloidal gold particles with anti–E-cadherin IgG or Fab could not be captured by OT for unknown reasons. We have noted that gold particles cannot be captured when coated with some mAbs. This is a major reason why we used L210 for the dragging experiments. An added benefit of using L210 was that the maximal trapping force with L210 was greater than that with G40 by a factor of  $\sim 3$ .

In our previous experiments of dragging receptors for transferrin and  $\alpha 2$ -macroglobulin, the results obtained by these two types of probes were basically the same (Sako and Kusumi, 1995). We also found that characteristics of diffusion for G40 and L210 attached to either transferrin receptor or  $\alpha 2$ -macroglobulin receptor were the same, except that the diffusion rate of G40-labeled receptors is  $\approx 20\%$  greater than that of L210-labeled receptors. In the present investigation, characteristics of diffusion of Wild labeled with G40-Fab or L210-IgG were found to be similar to each other. For all types of cadherin molecules, diffusion properties were the same for G40-IgG and G40-Fab as shown later (see below; and see Table II *b*). Therefore, the results of the dragging experiment would have been similar for G40-Fab and L210-IgG if G40 could have been used for dragging experiments. However, due caution in terms of the effect of cross-linking of cadherin molecules is required in interpreting the present data.

Transferrin receptor molecules tethered to the membrane skeleton/cytoskeleton network could be clearly distinguished from free transferrin receptor molecules by dragging them with OT (Sako and Kusumi, 1995). Membrane protein molecules tethered to the cytoskeleton or the membrane skeleton may be dragged only short distances (Fig. 1 *A*, right), and after escaping from OT, they may return to their initial positions before being dragged. On the other hand, membrane proteins that are free from the tether of the cytoskeleton may be dragged much further. Even if they encounter the membrane skeleton fence in the dragging path, they can pass through the fence if the trapping force is sufficiently strong (Fig. 1 *B*, right). In the case of transferrin receptor in the plasma membrane of NRK cells, half of the particles passed across the mem-

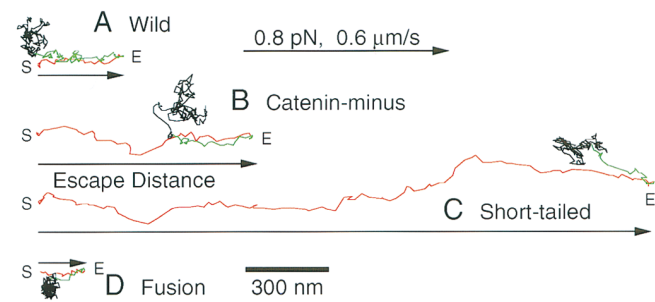


**Figure 4.** Trajectories of particle–cadherin complexes dragged by OT. E-cadherin and its mutants in the plasma membrane of living cells were labeled with 210-nm latex particles and dragged by OT. Trajectories of dragged particles for which the escape distance was the median value for each type of molecule are shown. The particles were dragged up to 5  $\mu\text{m}$  by moving the laser beam of the OT at a rate of 0.6  $\mu\text{m/s}$ . The maximal trapping force was 0.8 pN. The particles to be dragged were selected randomly on the free cell surface outside the cell–cell contact region. The directions for dragging were also randomly selected. In this figure, trajectories are arranged so that they start from the left and dragging proceeds to the right. Dragging was started at the point *S*, and the dragged portion is shown in red. The distance from the start position to the farthest point the particle reached by dragging (*E*, escape point) is called the escape distance (arrows). Many E-cadherin molecules showed rebound motion toward the initial positions after they escaped from the OT. The rebound is shown in green. After rebound motion, particles resumed random movements (black).

brane skeleton fence at a trapping force of 0.05–0.1 pN. If the trapping force was insufficient, the molecules tended to escape from the OT at the fence (Fig. 1 *B*, center).

Fig. 4 shows typical trajectories of E-cadherin during dragging and after escape from the OT. The distance from the initial trap point to the farthest point reached by the particle in OT dragging was measured, and is called “escape distance ( $d_{\text{esc}}$ )” in this report.

The time course of a typical dragging experiment is shown in Fig. 5 *A*. The displacements of a particle–cadherin complex and the center of the OT are plotted against time after the start of dragging. The OT was moved along the sample plane at a constant rate (0.6  $\mu\text{m/s}$ ). If the only force that is exerted on the complex besides that from the OT is hydrodynamic drag in the lipid bilayer, the force from the plasma membrane is small and the complex follows the OT. In the case shown in Fig. 5 *A*, the complex more or less followed for OT for up to 1.4 s from the start of dragging, or up to 0.78  $\mu\text{m}$ . After 1.4 s, the complex started to lag behind OT, indicating that some additional force from the cell started to act on the complex. This additional force is likely to be due to the membrane skeleton/cytoskeleton. In this report, the distance the complex followed the OT with little lag is called the “freely dragged distance ( $d_{\text{fd}}$ ).” As described below, the freely dragged distance is different from the “barrier-free path” (BFP, the distance from the start point to the farthest point reached by the particle with dragging) defined by Edidin et al. (1991).

The lag of the complex behind the center of the OT increased up to 2.8 s, at which point the complex escaped from the OT. At the escape point, the force exerted by the

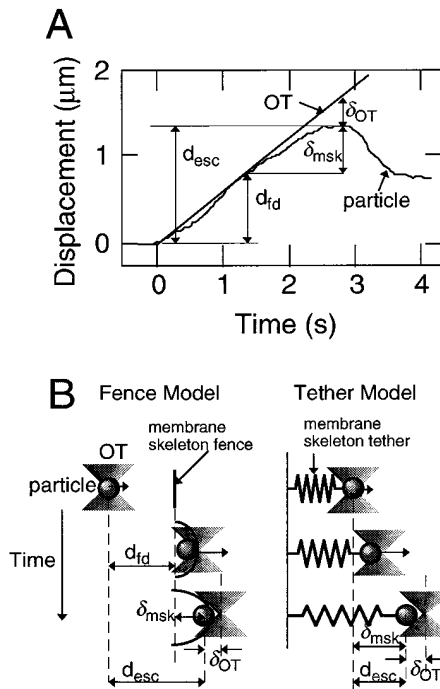


**Figure 5.** (A) The time course of a representative dragging experiment. The displacement of the particle and the center of the OT are plotted against time.  $d_{esc}$  represents the escape distance, and  $\delta_{OT}$  is the distance between the particle and the center of the OT at the escape point. Other parameters are explained in B. See the text for details. (B) Schematic drawings of the dragging experiments showing the interaction between the membrane protein and the membrane skeleton for the fence and tether models.  $d_{fd}$  represents the freely dragged distance, and  $\delta_{msk}$  represents the strain of the membrane skeleton/cytoskeleton at the escape point. See the text for details.

OT becomes the maximum value of 0.8 pN. Since the distance from the start point to the escape point is the escape distance, the escape distance in this report is the same as the BFP in Edidin et al. (1991), but at the maximum dragging force of 0.8 pN. In the experiment shown in Fig. 5 A, the escape distance is 1.32  $\mu\text{m}$ . In principle, the freely dragged distance is not dependent on the trapping force, whereas the escape distance is.

### Escape Distance and Freely Dragged Distance

Histograms of the escape distance are shown in Fig. 6. Fusion exhibited very short escape distances (Figs. 3 D and 5 D; and Table I). In contrast, E-cadherin mutants that lacked the catenin-binding domain (Catenin-minus and Short-tailed) could be dragged an average of  $>1 \mu\text{m}$  (mean; Figs. 6, B and C; and Table I). In particular, Short-tailed could be dragged farthest.

The distributions of the freely dragged distance for cadherins are shown in Fig. 7. E-cadherin molecules that are not bound to the membrane skeleton/cytoskeleton are expected to be dragged freely until they encounter the compartment boundaries (Fig. 5 B, left). On the other hand, cadherin molecules that are bound to the cytoskeleton must start to lag behind the OT immediately after the initiation of dragging (Fig. 5 B, right).

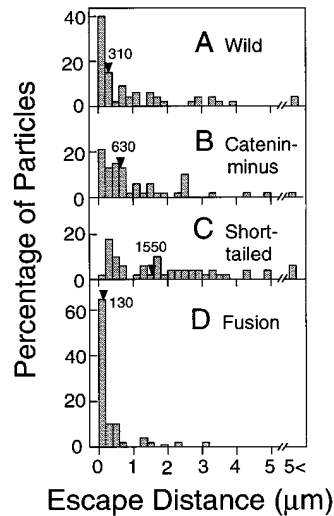


**Figure 6.** Distributions of the escape distances. The median values are indicated by arrowheads. The numbers of particles examined were 55 (A, Wild), 49 (B, Catenin-minus), 54 (C, Short-tailed), and 49 (D, Fusion).

The freely dragged distance for Fusion was only 20 nm (median), whereas Catenin-minus and Short-tailed showed much greater freely dragged distances (Fig. 7, note the logarithmic scale for the abscissa). In many cases (80%), Fusion started to lag behind the OT immediately after the start of dragging ( $d_{fd} < 50 \text{ nm}$ ). Some particles showed freely dragged distances  $< 10 \text{ nm}$  as seen in Fig. 6. Since our time resolution is limited to 33 ms, which reduces spatial resolution of a moving particle, the extremely short dragged distances simply indicate that the dragged distance was very small, or the backward movement induced by the force from the cell was initiated very early during dragging, and superimposed in the first several video frames. (Instrumental spatial precision is 1.5 nm.)

On the other hand, 65 and 82% of Catenin-minus and Short-tailed showed freely dragged distances of  $> 50 \text{ nm}$ , respectively. Freely dragged distances for Short-tailed were generally much greater than those for Catenin-minus. The cytoplasmic domain of Short-tailed (21-aa long) is substantially smaller than that of Catenin-minus (116-aa long). Therefore, the data on freely dragged distances are consistent with the membrane skeleton fence model, since Short-tailed should collide with the membrane skeleton fences less often than Catenin-minus.

These results are consistent with previous observations suggesting that the COOH-terminal region of  $\alpha$ -catenin is responsible for linking E-cadherin to actin filaments (Nagafuchi et al., 1994; Rimm et al., 1995). The binding affinity between  $\alpha$ -catenin and F-actin must be high because almost all of the Fusion molecules exhibited the characteristics of a tethered molecule.

The escape distances for Wild showed a broad distribution (Fig. 6 A). About half (58%) of Wild could be dragged  $< 400 \text{ nm}$ , whereas many (34%) Wild molecules could be dragged  $> 1 \mu\text{m}$ . These results suggest that there are two populations of Wild; one is tethered to the cytoskeleton and the other is not.

The distribution of the freely dragged distance for Wild (Fig. 7 A) also suggests the presence of two populations. About half (45%) of Wild showed freely dragged distances  $< 50 \text{ nm}$ , whereas  $\sim 1/3$  of Wild could be freely dragged  $> 500 \text{ nm}$ . This result again suggests that about

**Table I. The Median and Mean Values for the Escape Distance and the Freely Dragged Distance for E-Cadherin and Its Artificial Mutants (nm)**

Molecule	Escape distance		Freely dragged distance		Number of particles	>5 $\mu\text{m}^*$
	Median	(Mean $\pm$ SD)	Median	(Mean $\pm$ SD)		
Wild	310	(850 $\pm$ 1,070)	60	(670 $\pm$ 1,030)	53	2
Catenin-minus	630	(1,080 $\pm$ 1,130)	180	(610 $\pm$ 670)	48	1
Short-tailed	1,550	(1,760 $\pm$ 1,340)	1,070	(1,220 $\pm$ 1,110)	51	3
Fusion	130	(390 $\pm$ 640)	20	(190 $\pm$ 460)	49	0

\*Number of particles dragged to the end of the scan of the OT. Particles dragged to the end were excluded to obtain the mean and median values. The scanning velocity was 0.6  $\mu\text{m/s}$  and the maximum trapping force of the OT was 0.8 pN.

half of Wild is tethered to the cytoskeleton, while the other half is free and only confined by the presence of membrane skeleton corrals.

### Elasticity of the Membrane Skeleton/Cytoskeleton Network that Interacts with E-Cadherins

In the dragging experiments, many E-cadherin molecules showed rebound motion toward their initial positions after they escaped from the OT (Fig. 4), which indicates that the barriers for lateral dragging of E-cadherin are elastic. The elasticity of the membrane skeleton/cytoskeleton with which E-cadherins interact was estimated based on the response to the dragging by OT.

First, the distance from the point of initial encounter of E-cadherin with the membrane skeleton fence to the point at which E-cadherin escaped from the trap was measured. This distance is the same as the extension (strain) of the membrane skeleton, and called  $\delta_{\text{msk}}$  in the present paper, i.e.,  $\delta_{\text{msk}} = d_{\text{esc}} - d_{\text{fd}}$  (Fig. 5 B). For example,  $\delta_{\text{msk}}$  is 0.54  $\mu\text{m}$  in the case of Fig. 5 A.

The maximum trapping force of the OT used in the dragging experiments was 0.8 pN. Since this force equals the force from the membrane skeleton, at the escape

point, 0.8 (pN) =  $k_{\text{msk}} \times \delta_{\text{msk}}$ , where  $k_{\text{msk}}$  is the effective spring constant of the membrane skeleton/cytoskeleton with which the particle-cadherin complex was interacting. In this expression, the elasticity of the membrane skeleton is approximated by a simple spring. This assumption is good for small extension of the cytoskeleton, and has been found to be true in the case of red blood cells for the extent of deformation seen in the present experiment (Kusumi et al., 1997). The same Hookean expression can be used for E-cadherin molecules attached to the skeleton and those corralled by the skeleton. In the latter case, the origin is simply shifted to the point of initial encounter of the E-cadherin molecule to the membrane skeleton fence, whereas in the former case, the origin is the point where dragging was initiated.  $k_{\text{msk}}$  is 1.5 pN/ $\mu\text{m}$  in the case shown in Fig. 5 A.

It is important to realize that, in the present method,  $k_{\text{msk}}$  is estimated only when the particle escaped from the OT. In addition, since it is possible that more than one membrane skeleton fence is encountered during dragging of the distance  $\delta_{\text{msk}}$ , the estimated value of  $k_{\text{msk}}$  should be understood as the maximal estimate for the  $k_{\text{msk}}$  of the membrane skeleton fence.

Histograms of  $k_{\text{msk}}$ 's are shown in Fig. 8. Fusion exhibited  $k_{\text{msk}}$ 's greater than those for Catenin-minus and Short-tailed. Again, the distribution of Wild falls between these two extreme distributions.

It is likely that the force exerted on Short-tailed molecules from the membrane skeleton as they encounter during dragging is smaller than that on other E-cadherin. In the present investigation, we did not intend to measure such force. We only measured  $k_{\text{msk}}$  in the case where a particle escaped from the optical trap (in which case the escape force was 0.8 pN). To measure the dragging force required to move E-cadherin over the fence, particularly for E-cadherin with smaller cytoplasmic domains, much more refined method and instrumentation are required because the method has to be sensitive to all encounters of E-cadherin with the membrane skeleton fence, including those that involve very small force.

In Fig. 9,  $k_{\text{msk}}$  is plotted as a function of the freely dragged distance for each particle.  $k_{\text{msk}}$  of the tether for Fusion is broadly distributed (1–100 pN/ $\mu\text{m}$ ). However,  $k_{\text{msk}}$  for Fusion that exhibited freely dragged distances of <50 nm tended to be greater than that for Fusion that exhibited freely dragged distances of >50 nm.  $k_{\text{msk}}$  for Short-tailed was distributed in the range of 1–10 pN/ $\mu\text{m}$ , and there seemed to be no evident relationship between  $k_{\text{msk}}$  and the freely dragged distance for Short-tailed. The plot

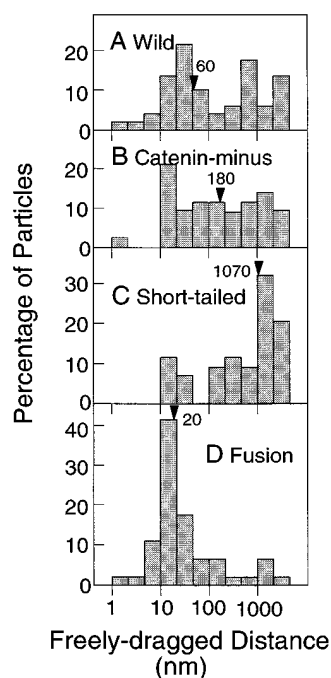


**Figure 7.** Distributions of the freely dragged distances. The median values are indicated by arrowheads. The numbers of particles examined were 53 (A, Wild), 48 (B, Catenin-minus), 51 (C, Short-tailed), and 49 (D, Fusion). The numbers of particles are different from those in Fig. 6, since the freely dragged distance cannot be determined in cases where particles are dragged to the end (5  $\mu\text{m}$ ) without any detectable lag. Note that the abscissa is shown on a log scale.

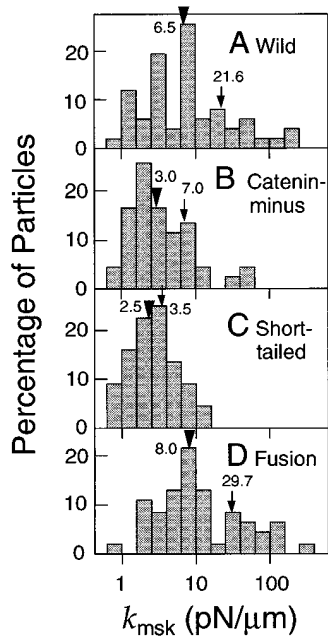


**Figure 8.** Distributions of the effective spring constant ( $k_{msk}$ ) of the portions of the membrane skeleton/cytoskeleton that are involved in corralling or tethering E-cadherin molecules. The mean and median values are indicated by arrows and arrowheads, respectively. Note that  $k_{msk}$  is plotted on a log scale.

for Wild looks like a mixture of those for Short-tailed and Fusion. The distribution of  $k_{msk}$  for Catenin-minus is similar to that for Short-tailed, although more points were in the region of a short, freely dragged distance, and some points in this region showed somewhat greater values for  $k_{msk}$ .

These results indicate that the cytoskeleton to which cadherins bind has greater effective spring constants than the membrane skeleton that is involved in corralling of cadherin molecules.  $k_{msk}$  for Fusion is likely to reflect the spring constant of the cytoskeleton to which cadherin is bound, and is estimated to be  $\sim 30$  pN/μm (Fig. 8 D). The maximal values of  $k_{msk}$  of the membrane skeleton, which acts like a picket fence for dragging of cadherin can be estimated from those found in the dragging of Short-tailed and Catenin-minus, and was found to be 3.5–7.0 pN/μm (Fig. 8, B and C). This result suggests that  $k_{msk}$  of the cytoskeleton that tethers E-cadherin is greater than that of the general membrane skeleton by a factor of more than six (comparison in terms of median values).

### Diffusion of E-Cadherins Observed by SPT

Movements of E-cadherins were followed by SPT. E-cadherin molecules on the cell surface were labeled with 40-nm gold particles through monoclonal anti-E-cadherin antibody (ECCD-2), and movements of individual gold particles were observed by video-enhanced differential interference contrast microscopy (Kusumi et al., 1993). Diffusion theories predict that simple increase in mass of the Brownian particles does not affect the diffusion rate (Berg, 1993). As long as the size of the particles are within the range of Brownian particles, the diffusion rate is determined by the balance between the hydrodynamic dragging force, which is dependent on the surface area (or radius, or their equivalents), and thermal agitation (kT) (Berg, 1993; Saffman and Delbrück, 1975). In addition, since the viscosity of lipid bilayers is greater than that of water by a factor

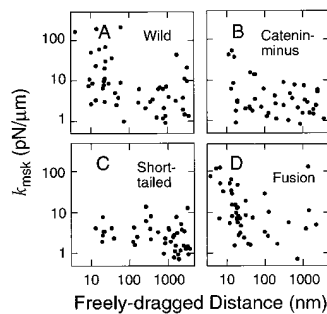


**Figure 9.**  $k_{msk}$  (effective spring constant) plotted against the freely dragged distance ( $d_{fd}$ ) for individual particles. Spring constants were calculated from the maximal trapping force of the OT (0.8 pN) and the strain ( $\delta_{msk}$ ; see Fig. 5) of the membrane skeleton/cytoskeleton. Note that both  $k_{msk}$  and the freely dragged distance are plotted on a log scale.

of about 100, the diffusion rate (more specifically, hydrodynamic dragging force) is mainly determined by the membrane-spanning domain unless there are other specific interactions such as those between the membrane protein and the membrane skeleton. Therefore, simple increase of the size of the extracellular domain by addition of G40 or L210 would not greatly affect the diffusion rate. In fact, in the present experiment, diffusion properties of Wild were the same for both G40 and L210 particles. Previously, we found that diffusion rates of transferrin receptor and  $\alpha 2$ -macroglobulin receptor decreased only 20% when the probe was changed from G40 to L210 (Sako and Kusumi, 1994). Diffusion rates of lipids in various cells and liposomes measured with G40 were practically the same as those measured by fluorescence redistribution after photobleaching (Lee et al., 1991; Kusumi, A., unpublished observations). In the present study, since all cadherin molecules used have the same extracellular and membrane-spanning domains, the difference in diffusion characteristics (and in responses to the dragging force exerted by laser tweezers) for different cadherins could be ascribed to changes induced by different cytoplasmic domains of these cadherins.

Typical trajectories observed by SPT for 16.7 s (500 video frames) are shown in Fig. 10. These trajectories are those that showed median MSD values at 5 s for each type of molecule (see the Materials and Methods). The area the movements covered was largest for Short-tailed, and smallest for Fusion.

The microscopic diffusion coefficient  $D_{micro}$  for each particle was calculated from MSD during 67–167 ms (see Materials and Methods), which represents the diffusion rate in this time window and a space scale of <500 nm. Fig. 11 shows the distributions of  $D_{micro}$ , and their mean and median values are listed in Table II.

$D_{micro}$  for Fusion shows a peak of  $\sim 2 \times 10^{-12}$  cm<sup>2</sup>/s (Fig. 11 D), which may represent local and/or fluctuating movements of the cytoskeleton to which Fusion is bound. Aggregation of Fusion molecules may occur through a putative self-assembly domain of  $\alpha$ -catenin (Nagafuchi et al., 1991), or through self-association of the extracellular domain of E-cadherin (Shapiro et al., 1995), but the dependence of the diffusion coefficients of membrane proteins on their size (i.e., aggregation) is slight (because the diffusion rate in a two-dimensional plane only depends on the logarithm of the radius of a diffusing unit; Saffman and Delbrück, 1975). If the difference in  $D_{micro}$  by a factor of 100 on average between Fusion and Short-tail were to be explained solely by aggregation of Fusion, the aggregate

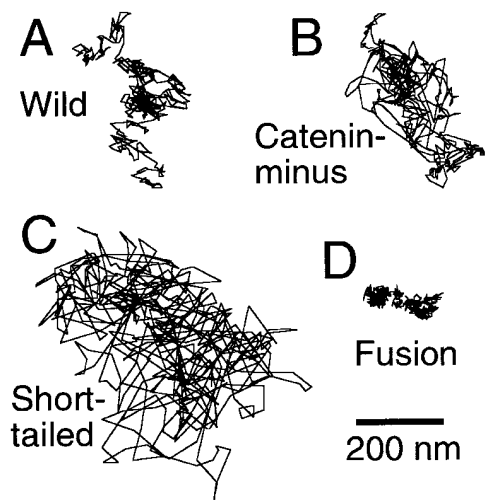


Figure 10. SPT trajectories of E-cadherins recorded for 16.7 s (500 video frames). Trajectories for which the 5-s MSD was the median value for each type of E-cadherin molecule are shown.

size of Fusion would have to be like  $>10,000$  monomers. Such large aggregates of Fusion molecules were not detected by indirect immunofluorescence microscopy (Figs. 3, D and H). These results suggest that the small  $D_{\text{micro}}$  (and short  $d_{\text{td}}$ ) for Fusion is mainly because of tethering to the cytoskeleton.

$D_{\text{micro}}$  values for Catenin-minus and Short-tailed exhibited peaks at  $\sim 0.9 \times 10^{-10}$  and  $\sim 3 \times 10^{-10}$   $\text{cm}^2/\text{s}$ , respectively, which are greater than that for Fusion by a factor of  $\sim 100$ . These results are consistent with the dragging data that suggest that Fusion was tethered to the cytoskeleton, whereas Catenin-minus and Short-tailed were not bound to the cytoskeleton. Only small subpopulations of Short-tailed and Catenin-minus showed  $D_{\text{micro}}$  values indicative of a bound component (Fig. 11, B and C). This may be due to binding to the cytoskeleton mediated by another membrane protein that is associated with the cytoskeleton.

The distribution of  $D_{\text{micro}}$  for Wild is broad, and covers the distributions for both Fusion and Catenin-minus (or Short-tailed). Wild molecules that exhibited  $D_{\text{micro}}$  values in the same range as Fusion molecules ( $<1.5 \times 10^{-11}$   $\text{cm}^2/\text{s}$ ) may be bound to the cytoskeleton, whereas those with  $D_{\text{micro}}$  values  $>1.5 \times 10^{-11}$   $\text{cm}^2/\text{s}$  are probably free from the cytoskeleton.

In conclusion, the distribution of  $D_{\text{micro}}$  for each cadherin represents a superposition of two populations. One may consist of molecules bound to the cytoskeleton and the other may consist of molecules free from the cytoskeleton. The bound and unbound fractions typically have  $D_{\text{micro}}$  values smaller or greater than  $\sim 1.5 \times 10^{-11}$   $\text{cm}^2/\text{s}$ , respectively.

Since gold particles can cross-link E-cadherin, and since the degree of cross-linking may vary from one type of cadherin to another because of different aggregation levels on the cell surface (although the aggregate size is small as shown in Fig. 3), SPT was performed with gold particles coated with anti-cadherin Fab with 1/5 molar amounts of IgG. The results of SPT are summarized in Table II b, which shows that the diffusion characteristics of gold-Fab

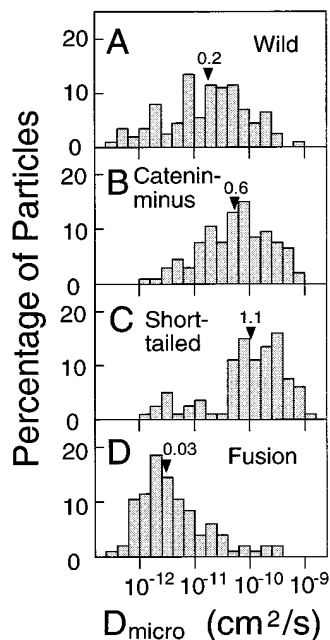


Figure 11. Distributions of  $D_{\text{micro}}$ . The median values are indicated by arrowheads ( $\times 10^{-10}$   $\text{cm}^2/\text{s}$ ).

particles are very similar to those of gold-IgG particles in all types of cells used in this work. In addition, diffusion characteristics of L210 bound to Wild are similar to those of G40-Fab and G40-IgG (data not shown). These results in turn suggest that these probes did not induce formation of large aggregates, and that the different diffusion characteristics observed for different cadherins were not created by cross-linking by the particle probes but were due to different cytoplasmic domains of these cadherins. As dis-

Table II. The Median and Mean Values for  $D_{\text{micro}}$  for E-Cadherin and Its Mutants, as Compared with Transferrin Receptor ( $10^{-10}$   $\text{cm}^2/\text{s}$ )

Molecule	Median	Mean $\pm$ SD	Number of particles
<i>a</i> IgG-G40			
E-Cadherin			
Wild	0.19	$0.52 \pm 0.90$	111
Catenin-minus	0.60	$1.24 \pm 1.57$	94
Short-tailed	1.14	$2.14 \pm 2.46$	81
Fusion	0.03	$0.19 \pm 0.56$	103
Transferrin Receptor			
ELB 1a (Cells expressing Wild)	0.35	$0.75 \pm 0.79$	47
ELB 24 (Cells expressing Short-tailed)	0.52	$0.93 \pm 0.76$	40
<i>b</i> Fab-G40			
E-Cadherin			
Wild	0.38	$0.43 \pm 0.42$	34
Catenin-minus	0.57	$1.03 \pm 1.61$	29
Short-tailed	1.34	$1.83 \pm 1.77$	29
Fusion	0.05	$0.16 \pm 0.31$	33
<i>c</i> IgG-G40, Cytochalasin D			
E-Cadherin			
Wild	0.014	$0.027 \pm 0.026$	18
Catenin-minus	0.045	$0.058 \pm 0.043$	18
Short-tailed	0.032	$0.036 \pm 0.016$	19
Fusion	0.022	$0.038 \pm 0.043$	20

Table III.  $D_{\text{micro}}$  ( $10^{-10}$  cm<sup>2</sup>/s), Drift Velocity (nm/s) and Confinement Area ( $\mu\text{m}^2$ ) for E-Cadherins Classified as Directed Movement and Confined Diffusion (Mean  $\pm$  SD)

Molecule	Directed movement			Confined diffusion		
	$D_{\text{micro}}$	Drift velocity	(n)*	$D_{\text{micro}}$	Confinement area	(n)*
E-Cadherin						
Wild	0.04 $\pm$ 0.07	27.3 $\pm$ 28.3	(9)	0.71 $\pm$ 0.76	0.16 $\pm$ 0.19	(38)
Catenin-minus	NA <sup>‡</sup>	NA		1.42 $\pm$ 1.63	0.14 $\pm$ 0.22	(46)
Short-tailed	NA	NA		1.86 $\pm$ 2.18	0.50 $\pm$ 0.80	(38)
Fusion	0.03 $\pm$ 0.03	20.3 $\pm$ 14.1	(21)	NA	NA	
Transferrin Receptor						
EL $\beta$ 1a (Cells expressing Wild)	NA	NA		0.66 $\pm$ 0.53	0.12 $\pm$ 0.05	(17)
EL $\beta$ 24 (Cells expressing Short-tailed)	NA	NA		0.74 $\pm$ 0.51	0.19 $\pm$ 0.19	(14)

\*Number of particles classified as directed or confined diffusion.

<sup>‡</sup>NA, not applicable. Statistically meaningless numbers of particles exhibited these motional modes.

cussed previously, most of the IgG and Fab molecules on the surface of the gold or latex particles are likely to be denatured, which reduces the effective valency of these particle probes (Sako and Kusumi, 1994; Kusumi et al., 1997).

In some trajectories, they show behaviors that suggest interconversion of bound and unbound states. However, since diffusion is a stochastic process, it is very difficult to prove that the particular changes observed in a trajectory is statistically meaningful. At this stage of the investigation, we would like to refrain from making specific comments on these. However, we would like to point out the possibility that the spread in  $D_{\text{micro}}$  for Wild seen in Fig. 11 could partially be due to interconversion between the free and the bound states. Another possible reason for the spread in  $D_{\text{micro}}$  could be because of coexistence of particles that are bound to different number of E-cadherin molecules.

Movements of transferrin receptor in transfectants expressing Wild (EL $\beta$  1a) and Short-tailed (EL $\beta$  24) were observed by SPT (Tables II and III).  $D_{\text{micro}}$  and the confinement area (see below) for transferrin receptor were similar in both clones, indicating that the differences observed among various E-cadherins depend on the structural differences in their cytoplasmic domains, rather than on differences in cellular structures.

Although most of the Catenin-minus and Short-tailed molecules appear to be free from tethering to the cytoskeleton,  $D_{\text{micro}}$  for these molecules ( $1\text{--}2 \times 10^{-10}$  cm<sup>2</sup>/s) was smaller than that expected for membrane proteins diffusing freely in the plasma membrane ( $1\text{--}4 \times 10^{-9}$  cm<sup>2</sup>/s; Jacobson et al., 1987), i.e.,  $D_{\text{micro}}$  of E-cadherin is reduced by mechanisms other than long-term binding to the cytoskeleton.  $D_{\text{micro}}$  for transferrin receptor was 10-fold smaller in L cells ( $\sim 10^{-10}$  cm<sup>2</sup>/s; Table II) than in NRK cells ( $\sim 10^{-9}$  cm<sup>2</sup>/s; Sako and Kusumi, 1994). The mechanism that reduces  $D_{\text{micro}}$  of these proteins in the plasma membrane of L cells is not known. This reduction may be because of a crowding effect by other membrane proteins, particularly in their extracellular domains (Sheetz, 1993), interaction with the extracellular matrix (Lee et al., 1993), and/or a percolation effect of immobile or slowly diffusing obstacles (Saxton, 1987). The association of a cadherin-catenin complex with other proteins has been reported (Balsamo and Lilien 1990; Nelson, et al., 1990; Itoh et al., 1993; Hinck et al., 1994; Hoschuetzky et al., 1994).

### Directed Movements of E-Cadherins Bound to the Cytoskeleton

Movements of E-cadherin observed by SPT were statistically classified into three types of motion, i.e., simple diffusion, confined diffusion, and directed movement (Kusumi et al., 1993), within a time window of 5 s. The results are shown in Fig. 12 with further classification; values for  $D_{\text{micro}}$  greater or smaller than  $1.5 \times 10^{-11}$  cm<sup>2</sup>/s correspond to mostly unbound and bound cadherin molecules, respectively (as discussed in the previous section).

Considerable fractions of Wild and Fusion undergo directed movement (8 and 20%, respectively; Table III). On the other hand, Catenin-minus and Short-tailed did not show directed movement. (Because of the statistical nature of this classification method, a percentage of <2.5 for directed movement is insignificant, see Materials and Methods.) Representative trajectories of particles classified as directed movement are shown in Fig. 13, *A* (Wild) and *B* (Fusion). Such movements of Wild and Fusion reflected the superposition of rather linear and uniform motion and random diffusion, in which  $D_{\text{micro}}$  was smaller than the overall average by a factor of 6–13 (Table II and III). The average drift velocity was  $\sim 20\text{--}30$  nm/s (Table III), which is comparable to the velocity of the tread milling of actin filament in the cytoplasm (Wang, 1985; Sheetz et al., 1989). These properties suggest that directed movement is related to the movement of cytoskeletal filaments rather than to membrane flow.

### Confined Diffusion of Unbound E-Cadherins

A large fraction (30–40%) of Wild, Catenin-minus, and Short-tailed molecules exhibited confined diffusion, as shown in Fig. 12. This mode is more clearly seen in the population that showed  $D_{\text{micro}}$  values  $> 1.5 \times 10^{-11}$  cm<sup>2</sup>/s (50%).

We previously proposed that the compartmentalized structure caused by the membrane skeleton fence is a basic feature of the plasma membrane (Kusumi and Sako, 1996). According to this model, particles that are classified as exhibiting simple diffusion are undergoing “apparently simple diffusion.” They may be located in larger compartments and/or have smaller  $D_{\text{micro}}$  values. For example, in the time scale used for classifying the mode in this report (5 s), particles exhibiting  $D_{\text{micro}}$  values  $< 0.75 \times 10^{-10}$  cm<sup>2</sup>/s

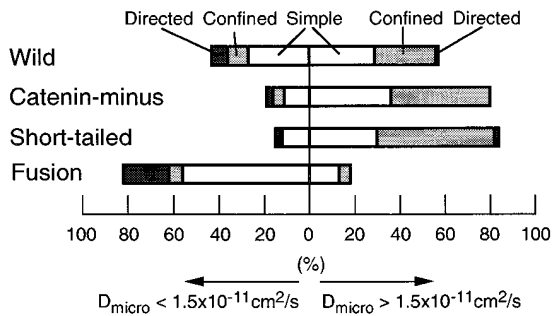


**Figure 12.** Classification of trajectories into simple Brownian, confined, and directed movement modes in a time window of 5 s. The results are shown separately for  $D_{\text{micro}}$  values greater and smaller than  $1.5 \times 10^{-11} \text{ cm}^2/\text{s}$ .

will not feel the boundaries of compartments that are  $>0.15 \mu\text{m}^2$ , which is the average compartment size for Wild and Catenin-minus (Table III). This may explain why few particles with  $D_{\text{micro}}$  values  $<1.5 \times 10^{-11} \text{ cm}^2/\text{s}$  are classified into the confined diffusion mode (Fig. 12). Therefore, for the movements of cadherins that are not bound to the cytoskeleton, compartmentalization of the plasma membrane, perhaps because of membrane skeletal barriers, plays a major role in determining their mobility.

The confinement area was the same for Wild, Catenin-minus, and transferrin receptor ( $0.15 \mu\text{m}^2$  on average), but was greater ( $0.5 \mu\text{m}^2$ ) for Short-tailed, which has a very small cytoplasmic domain (21 aa) (Table III). These results support the notion that the membrane skeleton fence effect is a mechanism for regulating the diffusion of cadherins that are not bound to the cytoskeleton.

### Effect of Cytochalasin D on E-Cadherin Diffusion

SPT measurements were carried out in the presence of  $1 \mu\text{M}$  cytochalasin D to examine the effect of partial destruction of actin filaments. The effect was dramatic and almost all particles started undergoing slow simple Brownian diffusion after the drug treatment.  $D_{\text{micro}}$  decreased by a factor of 10–50 except for Fusion, which showed a decrease by a factor of 2.5 (Table II c). Although these results do not directly support the fence or the tether models, they strongly suggest the involvement of actin filaments in regulation of the movement of cadherin. Such reduction of  $D_{\text{micro}}$  and increase in the simple Brownian mode in the cells treated with cytochalasin D were previously observed for receptors for transferrin and  $\alpha 2$ -macroglobulin in NRK cells (Sako and Kusumi, 1994). It is possible that membrane proteins were trapped in the membrane-bound aggregates of actin filaments formed by the cytochalasin treatment.

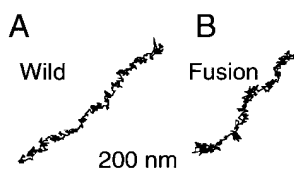


**Figure 13.** Typical trajectories of Wild (A) and Fusion (B) classified as directed movement. Recording time was 16.7 s (500 video frames).

## Discussion

### Cytoplasmic Regulation of the Movements of E-Cadherin in the Plasma Membrane by the Membrane Skeleton/Cytoskeleton Network

Based on motion analysis by SPT and lateral dragging by OT of transferrin receptor,  $\alpha 2$ -macroglobulin receptor, EGF receptor, and E-cadherin, we have proposed two mechanisms for the cytoplasmic regulation of movements of membrane proteins in the plasma membrane, i.e., tethering to the cytoskeleton and temporal confinement within the membrane skeleton mesh (Fig. 1; Kusumi and Sako, 1996). The results of other groups have also suggested the cytoplasmic regulation of the movement of plasma membrane proteins by the membrane skeleton/cytoskeleton network (Sheetz et al., 1980, 1989; Kucik et al., 1989; De Brabander et al., 1991; Edidin and Stroynowski, 1991; Schmidt et al., 1993; Wang et al., 1994). In the present study, we examined the cytoplasmic regulation of E-cadherin using the wild type and three cytoplasmic mutants.

Fig. 14 shows a model which we propose to explain the results obtained in this research. Tethering to the cytoskeleton, as shown in Fig. 14 A, was typical of Fusion. The small  $D_{\text{micro}}$  for Fusion may reflect the local movement and conformational fluctuation of the cytoskeleton to which Fusion is bound. In addition, some of the tethered molecules are transported directly. Catenin-minus and Short-tailed do not exhibit tethering to the cytoskeleton, but are confined within submicrometer scale membrane compartments (Fig. 14, C and D, respectively). A decrease in the size of the cytoplasmic domain of E-cadherin from 116 aa (Catenin-minus) to 21 aa (Short-tailed) produces an increase in the compartment size by a factor of four (Table III). The possibility of colliding with the fence of the membrane skeleton network should be greater for a molecule with a greater cytoplasmic domain.

The results for Wild suggest the presence of two populations of Wild: one that is tethered to the membrane skeleton/cytoskeleton and another that is unbound but confined by the membrane skeleton (Fig. 14, A–C). About half of Wild showed an escape distance (Fig. 6) and a freely dragged distance (Fig. 7) as short as those for Fusion, whereas the other half showed values similar to those for Catenin-minus and Short-tailed. In addition, the distribution of  $D_{\text{micro}}$  for Wild appeared to be a superposition of those for Fusion ( $10^{-12}$ – $1.5 \times 10^{-11} \text{ cm}^2/\text{s}$ ) and Short-tailed ( $1.5 \times 10^{-11}$ – $10^{-9} \text{ cm}^2/\text{s}$ ) (Fig. 11).

Similar SPT and OT experiments were carried out with other mutants of E-cadherin that have a deletion inside (aa 814–849; EL $\beta$  32) or outside (aa 774–813, EL $\beta$  33; and aa 751–773, EL $\beta$  34) of the catenin-binding domain (Nagafuchi and Takeichi, 1989). The results are summarized in Table IV.  $D_{\text{micro}}$  is expected to be smaller for mutants with actin-binding capability (i.e., with catenin-binding sites), which was observed.  $D_{\text{micro}}$  for EL $\beta$  32 is close to catenin-minus, whereas those for EL $\beta$  33 and 34 are similar to Wild. Confinement areas for the particles undergoing confined diffusion are similar to Wild and Catenin-minus, which is also consistent with the above model. Escape distance was only measured with EL $\beta$  33, and found

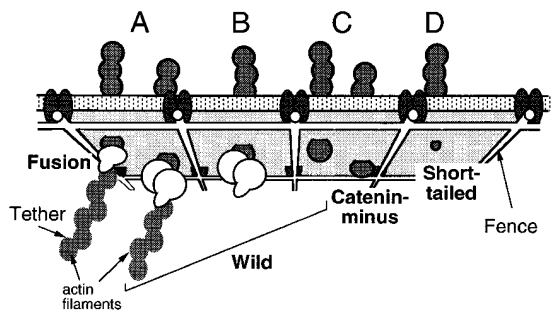


**Figure 14.** Models of the mechanisms for the regulation of the movement of E-cadherins in the plasma membrane. Movements are regulated through the cytoplasmic domain of E-cadherin by the tethering and corraling effects of the membrane skeleton/cytoskeleton network. Most of the Fusion molecules are tethered to the cytoskeleton through the COOH-terminal domain of  $\alpha$ -catenin (A, left). Catenin-minus and Short-tailed are free from tethering, but exhibit temporarily confined diffusion within submicrometer-scale membrane compartments bounded by the membrane skeleton (C, right and D, respectively). A decrease in the size of the cytoplasmic domain increases the probability that cadherin will pass the fence (D). Wild has two populations; about half is tethered to the cytoskeleton (A, right), whereas the other half is corralled in the membrane skeletal mesh (B and C, left).

to be  $\sim 200$  nm, which is close to Wild. This again is consistent with the above model.

We found a submicron scale meshwork on the cytoplasmic surface of the dorsal part of the plasma membrane, much of which was consisted of actin filaments (Kawasaki et al., 1995). Actin filaments may be involved in the membrane skeleton fence structure that restricts the movement of E-cadherin within compartments, consistent with the effect of cytochalasin D. The cytoskeleton to which E-cadherin is tethered is likely composed of actin filaments (Hirano et al., 1987; Nagafuchi and Takeichi, 1989; Ozawa et al., 1990).

$\alpha$ -Catenin has been proposed to mediate E-cadherin-actin linkage (Nagafuchi and Takeichi, 1989; Ozawa et al., 1989, 1990). The COOH-terminal half of  $\alpha$ -catenin possesses regions that are homologous to the actin-binding region of vinculin (Nagafuchi et al., 1994; Johnson and Craig, 1995). Recently, the COOH-terminal part of  $\alpha$ -catenin consisting of 447 aa was reported to bind directly to F-actin (Rimm et al., 1995). On the other hand, a yeast two-hybrid assay and an in-vitro binding assay between recombinant E-cadherin and catenins have suggested that  $\beta$ -catenin mediates the association between E-cadherin and  $\alpha$ -catenin (Jou et al., 1995).

#### **Activities of Cell-Cell Adhesion and of Actin Binding of E-Cadherin Are Highly Correlated**

In the cell aggregation assay, it was shown that Fusion has higher activity in inducing aggregation of cells. The cells expressing Fusion were found to be flat even in the metaphase of cytokinesis (Nagafuchi et al., 1994). These observations indicate that Fusion has greater cell adhesion activity than Wild.

The present results indicate that half of Wild molecules are free from tethering, whereas almost all of Fusion mole-

**Table IV.** Summary of OT and SPT Measurements of Other E-Cadherin Mutants

Molecule	Cytoplasmic domain aa	Catenin binding	$D_{\text{micro}}^*$ $10^{-10} \text{ cm}^2/\text{s}$	Area <sup>**</sup> $\mu\text{m}^2$	Escape distance <sup>§</sup> nm
EL $\beta$ 32	117	–	$1.34 \pm 1.39$	$0.15 \pm 0.29$	ND <sup>  </sup>
EL $\beta$ 33	116	+	$0.86 \pm 0.71$	$0.10 \pm 0.08$	200
EL $\beta$ 34	133	+	$0.50 \pm 0.72$	$0.19 \pm 0.28$	ND

\*Mean  $\pm$  SD.

\*\*Confinement area for the particles undergoing confined diffusion.

§Median value.

||ND, experiments not done.

cules are bound to the cytoskeleton. Since tethering to the cytoskeleton mediated by  $\alpha$ -catenin is necessary for E-cadherin to exhibit cell adhesion activity (Watabe et al., 1994), greater activity of Fusion can be explained by its binding to the actin skeleton.

Related to this correlation is the present finding that the spring constant of the membrane skeleton involved in tethering is greater than that involved in corraling by a factor of six. Actin bundles may be involved in tethering of E-cadherin, which may help strengthen the cell adhesion activities.

#### **Resistance to Detergent Extraction and Tethering to the Membrane Skeleton/Cytoskeleton**

Previous studies have assumed that most of the Wild and Fusion molecules located inside cell-cell contact regions could not be extracted by a nonionic detergent, 2.5% NP-40 (Nagafuchi and Takeichi, 1989; Nagafuchi et al., 1994) or a mixture of 1% NP-40 and 1% Triton X-100 (Ozawa et al., 1989, 1990). Although considerable amounts of E-cadherin molecules are diffusely distributed over the cell surface, it has been difficult to find out whether or not they are bound to the cytoskeleton. Such population of cadherin is important because these cadherins provide the ready pool for new cell-cell association, and perhaps they may be surveying new physical contacts with other cells. However, detergent extraction was incapable of distinguishing bound and unbound components of E-cadherin. Wild and Fusion molecules were largely extracted from the free cell surface with nonionic detergents as examined by immunofluorescence microscopy (Nagafuchi and Takeichi, 1989; Nagafuchi et al., 1994).

The SPT and OT experiments in the present study showed that half of Wild and most of Fusion are linked to the cytoskeleton, even outside cell-cell contact sites. This clearly shows that even membrane proteins that are bound to the cytoskeleton can be extracted by nonionic detergents, i.e., extractability with nonionic detergents is no guarantee for unbinding of the membrane protein from the cytoskeleton. Mechanical assays, such as SPT and OT, are more direct and reliable than detergent extraction methods.

#### **Mechanical Properties of the Interaction between Membrane Proteins and the Membrane Skeleton/Cytoskeleton Network**

Both the tether and fence structures interacting with E-cad-

herin could be deformed using OT at a dragging force of 0.8 pN, and rebound motion of E-cadherin after its escape from OT indicates that the tether and fence are elastic (Fig. 4). The median values for spring constants of the tether and fence estimated from the dragging experiments were 30 and 3.5 pN/ $\mu\text{m}$ , respectively (Fig. 8; 8 and 3 pN/ $\mu\text{m}$  on average). Previously, we found that the effective spring constants of the membrane skeleton involved in the tether and fence were  $\sim 12$  and 3 pN/ $\mu\text{m}$ , respectively, in a dragging experiment of transferrin receptor in NRK cells (Sako and Kusumi, 1995).

In both L (expressing E-cadherins) and NRK (transferrin receptor) cells, the effective spring constant for tethers is greater than that for fences, suggesting that the structure of the membrane skeleton and the cytoskeleton involved in these interactions are different. In the case of E-cadherin, tethers may be bundles of actin filaments, whereas fences may be thinner bundles or single actin filaments. The average fluctuation of the elastic filaments for tethers ( $k_{\text{msk}} = 0.03$  pN/nm) and fences ( $k_{\text{msk}} = 0.0035$  pN/nm) can be estimated from the elastic constants, and was found to be 10 and 30 nm, respectively [since  $(1/2)k_{\text{msk}} < x^2 > = (1/2)k_{\text{B}}T = 2$  pN $\cdot$ nm,  $< x^2 >^{1/2} = < 4/k_{\text{msk}} >^{1/2}$  nm].

One way to estimate fluctuation of the cytoskeleton is to examine the trajectories of directed movements, and evaluate the mean fluctuation perpendicular to the direction of drift movement (because the cytoskeleton is responsible for such directed movements). This was done using  $\text{MSD}_{150}$  in the perpendicular direction to the directed movement, and was found to be  $21 \pm 2$  and  $40 \pm 20$  nm for Wild and Fusion, respectively, in general agreement with those estimated from the spring constant. This agreement suggests again that the cytoskeleton is responsible for forming tethers and the fences for E-cadherin.

### Calcium-induced Assembly of E-Cadherin during the Formation of Adherens Junctions

In the course of the calcium-induced formation of cell-to-cell adherens junctions in epithelial cells in vitro, E-cadherin on the dorsal cell surface assembles into cell-cell contact sites. This assembly occurs via the movement of E-cadherin in the plasma membrane (Kusumi et al., 1988). Therefore, the mechanism that regulates the movement of E-cadherin on the cell surface is important for E-cadherin assembly and the formation of adherens junctions (McNeill et al., 1993).

E-cadherin in adherens junctions is linked to actin filaments (Hirano et al., 1987; Nagafuchi et al., 1994), whereas data by SPT and OT indicate that only part of the E-cadherin on the free cell surface (outside the cell-cell contact region) is associated with the cytoskeleton in both cultured mouse keratinocyte (Kusumi et al., 1993) and L cells. Regulation mechanisms, such as the binding of E-cadherin to the cytoskeleton, cytoskeleton-dependent transport of bound and corralled E-cadherin, and changes in the association states of E-cadherin, which would greatly affect binding and corraling of E-cadherin by the membrane skeleton, may play important roles in the assembly of E-cadherin at cell-cell contact sites.

Received for publication 29 July 1997 and in revised form 8 January 1998.

### References

- Ashkin, A., J.M. Dziedzic, J.E. Bjorkholm, and S. Chu. 1986. Observation of a single-beam gradient force optical trap for dielectric particles. *Optics Lett.* 11:288–290.
- Ashkin, A., J.M. Dziedzic, and T. Yamane. 1987. Optical trapping and manipulation of single cells using infrared-laser beams. *Nature.* 330:769–771.
- Bacallao, R., C. Antony, C. Dotti, E. Karsenti, E.H. Stelzer, and K. Simons. 1989. The subcellular organization of Madin-Darby canine kidney cells during the formation of a polarized epithelium. *J. Cell Biol.* 109:2817–2832.
- Balsamo, J., and J. Lilien. 1990. N-cadherin is stably associated with and is an acceptor for a cell surface N-acetylgalactosaminylphosphotransferase. *J. Biol. Chem.* 265:2923–2928.
- Berg, H.C. 1983. *Random Walks in Biology.* Princeton University Press, Princeton, New Jersey.
- De Brabander, M., G. Geuens, R. Nuydens, M. Moeremans, and J. De May. 1985. Probing microtubule-dependent intracellular motility with nanometer particle video ultramicroscopy (nanovid ultramicroscopy). *Cytobios.* 43: 273–283.
- De Brabander, M., R. Nuydens, A. Ishihara, B. Holifield, K. Jacobson, and H. Geerts. 1991. Lateral diffusion and retrograde movements of individual cell surface components on single motile cells observed with nanovid microscopy. *J. Cell Biol.* 112:111–124.
- Eididin, M., and I. Stroynowski. 1991. Differences between the lateral organization of conventional and inositol phospholipid-anchored membrane proteins. A further definition of micrometer scale domains. *J. Cell Biol.* 112: 1143–1150.
- Eididin, M., S.C. Kuo, and M.P. Sheetz. 1991. Lateral movements of membrane glycoproteins restricted by dynamic cytoplasmic barriers. *Science.* 254:1379–1382.
- Gelles, J., B.J. Schnapp, and M.P. Sheetz. 1988. Tracking kinesin-driven movements with nanometer-scale precision. *Nature.* 331:450–453.
- Hinck, L., I.S. N athke, J. Papkoff, and W.J. Nelson. 1994. Dynamics of cadherin/catenin complex formation: Novel protein interactions and pathways of complex assembly. *J. Cell Biol.* 125:1327–1340.
- Hirano, S., A. Nose, K. Hatta, A. Kawakami, and M. Takeichi. 1987. Calcium-dependent cell-cell adhesion molecules (cadherins): Subclass specificities and possible involvement of actin bundles. *J. Cell Biol.* 105:2501–2510.
- Hirano, S., N. Kimoto, Y. Shimoyama, S. Hirohashi, and M. Takeichi. 1992. Identification of a neural  $\alpha$ -catenin as a key regulator of cadherin function and multicellular organization. *Cell.* 70:293–301.
- Hoschuetzky, H., H. Aberle, and R. Kemler. 1994.  $\beta$ -Catenin mediates the interaction of the cadherin-catenin complex with epidermal growth factor receptor. *J. Cell Biol.* 127:1375–1380.
- Itoh, M., A. Nagafuchi, S. Yonemura, T. Kitani-Yasuda, Sa. Tsukita, and Sh. Tsukita. 1991. The 220-kD protein colocalizing with cadherins in non-epithelial cells is identical to ZO-1, a tight junction-associated protein in epithelial cells: cDNA cloning and immunoelectron microscopy. *J. Cell Biol.* 121:491–502.
- Jacobson, K., A. Ishihara, and R. Inman. 1987. Lateral diffusion of proteins in membranes. *Annu. Rev. Physiol.* 49:163–175.
- Johnson, R.P., and S.W. Craig. 1995. F-Actin binding site masked by the intramolecular association of vinculin head and tail domains. *Nature.* 373:261–264.
- Jou, T.-S., D.B. Stewart, J. Stappert, W.J. Nelson, and J.A. Marrs. 1995. Genetic and biochemical dissection of protein linkages in the cadherin-catenin complex. *Proc. Natl. Acad. Sci. USA.* 92:5067–5071.
- Kawasaki, K., Y. Sako, and A. Kusumi. 1995. Three-dimensional analysis of the membrane skeleton structure of cultured cells by atomic force microscopy. *Cell Struct. Funct.* 20:606.
- Kucik, D.F., E.L. Elson, and M.P. Sheets. 1989. Forward transport of glycoproteins on leading lamellipodia in locomoting cells. *Nature.* 340:315–317.
- Kusumi, A., and Y. Sako. 1996. Cell surface organization by the membrane skeleton. *Curr. Opin. Cell Biol.* 8:566–574.
- Kusumi, A., A. Tsuji, M. Murata, Y. Sako, A.C. Yoshizawa, T. Hayakawa, and S. Ohnishi. 1988. Development of a time-resolved microfluorimeter with a synchroscan streak camera and its application to studies of cell membranes. *SPIE Proc.* 909:350–351.
- Kusumi, A., Y. Sako, and M. Yamamoto. 1993. Confined lateral diffusion of membrane receptors as studied by single particle tracking (nanovid microscopy). Effects of calcium-induced differentiation in cultured epithelial cells. *Biophys. J.* 65:2021–2040.
- Kusumi, A., Y. Sako, T. Fujiwara, and M. Tomishige. 1997. Application of laser tweezers to studies of the fences and tethers of the membrane skeleton that regulate the movements of plasma membrane proteins. *Methods Cell Biol.* 55:174–194.
- Lee, G.M., A. Ishihara, and K.A. Jacobson. 1991. Direct observation of Brownian motion of lipids in a membrane. *Proc. Natl. Acad. Sci. USA.* 88:6274–6278.
- Lee, G.M., F. Zhang, A. Ishihara, C.L. McNail, and K. Jacobson. 1993. Unconfined lateral diffusion and an estimate of pericellular matrix viscosity revealed by measuring the mobility of gold-tagged lipids. *J. Cell Biol.* 120:25–35.
- McCrea, P.D., C.W. Truch, and B. Gumbiner. 1991. A homologue of the armadillo protein in *Drosophila* (plakoglobin) associated with E-cadherin. *Science.* 254:1359–1361.
- McNeill, H., T.A. Ryan, S.J. Smith, and W.J. Nelson. 1993. Spatial and temporal dissection of immediate and early events following cadherin-mediated

- epithelial cell adhesion. *J. Cell Biol.* 120:1217–1226.
- Mecham, R.P., L.Whitehouse, M. Hay, A. Hinek, and M.P. Sheetz. 1991. Ligand affinity of the 67-kD elastin/laminin binding protein is modulated by the protein's lectin domain: Visualization of elastin/laminin-receptor complexes with gold-tagged ligands. *J. Cell Biol.* 113:187–194.
- Nagafuchi, A., and M. Takeichi. 1988. Cell binding function of E-cadherin is regulated by the cytoplasmic domain. *EMBO (Eur. Mol. Biol. Organ.) J.* 12:3674–3684.
- Nagafuchi, A., and M. Takeichi. 1989. Transmembrane control of cadherin-mediated cell adhesion: a 94 kDa protein functionally associated with a specific region of the cytoplasmic domain of E-cadherin. *Cell Regul.* 1:37–44.
- Nagafuchi, A., M. Takeichi, and Sh. Tsukita. 1991. The 102-kDa cadherin-associated protein: similarity to vinculin and posttranscriptional regulation of expression. *Cell.* 65:849–857.
- Nagafuchi, A., S. Ishihara, and Sh. Tsukita. 1994. The roles of catenins in the cadherin-mediated cell adhesion: Functional analysis of E-cadherin- $\alpha$  catenin fusion molecules. *J. Cell Biol.* 127:235–245.
- Nelson, W.J., E.M. Shore, A.Z. Wang, and R.W. Hammerton. 1990. Identification of a membrane-cytoskeletal complex containing the cell adhesion molecule uvomorulin (E-cadherin), ankyrin, and fodrin in Madin-Darby canine kidney epithelial cells. *J. Cell Biol.* 110:349–357.
- Nose, A., A. Nagafuchi, and M. Takeichi. 1988. Expressed recombinant cadherins mediate cell sorting in model systems. *Cell.* 54:993–1001.
- Ozawa, M., H. Baribault, and R. Kemler. 1989. The cytoplasmic domain of the cell adhesion molecule uvomorulin associates with three independent proteins structurally related in different species. *EMBO (Eur. Mol. Biol. Organ.) J.* 8:1711–1717.
- Ozawa, M., M. Ringwald, and R. Kemler. 1990. Uvomorulin-catenin complex formation is regulated by a specific domain in the cytoplasmic region of the cell adhesion molecule. *Proc. Natl. Acad. Sci. USA.* 82:4246–4250.
- Peifer, M., S. Berg, and A.B. Reynolds. 1994. A repeating amino acid motif shared by proteins with diverse cellular roles. *Cell.* 76:789–91.
- Reynolds, A.B. and D.J. McCrea. 1994. Identification of a new catenin: the tyrosine kinase substrate p120 associates with E-cadherin complexes. *Mol. Cell. Biol.* 14:8333–8342.
- Rimm, D.L., E.R. Koslov, P. Kebriaei, C.D. Cianci, and J.S. Morrow. 1995.  $\alpha_1$ (E)-Catenin is an actin-binding and -bundling protein mediating the attachment of F-actin to the membrane adhesion complex. *Proc. Natl. Acad. Sci. USA.* 92:8813–8817.
- Saffman, P.B., and M. Delbrück. 1975. Brownian motion in biological membranes. *Proc. Natl. Acad. Sci. USA.* 72:3111–3113.
- Sako, Y., and A. Kusumi. 1994. Compartmentalized structure of the plasma membrane for lateral diffusion of receptors as revealed by nanometer-level motion analysis. *J. Cell Biol.* 125:1251–1264.
- Sako, Y., and A. Kusumi. 1995. Barriers for lateral diffusion of transferrin receptors in the plasma membrane as characterized by receptor dragging by laser tweezers: fence versus tether. *J. Cell Biol.* 129:1559–1574.
- Saxton, M.J. 1987. Lateral diffusion in an archipelago. The effect of mobile obstacles. *Biophys. J.* 52:989–997.
- Schmidt, C.E., A.F. Horwitz, D.A. Lauffenburger, and M.P. Sheetz. 1993. Integrin-cytoskeletal interactions in migrating fibroblasts are dynamic, asymmetric, and regulated. *J. Cell Biol.* 123:977–991.
- Shapiro, L., A.M. Fannon, P.D. Kwong, A. Thompson, M.S. Lehmann, G. Grübel, J.-F. Legrand, J. Als-Neilsen, D.R. Colman, and W.A. Hendrickson. 1995. Structural basis of cell-cell adhesion by cadherins. *Nature.* 374:327–337.
- Sheetz, M.P. 1993. Glycoprotein motility and dynamic domains in fluid plasma membranes. *Annu. Rev. Biophys. Biomol. Struct.* 22:417–431.
- Sheetz, M.P., M. Schindler, and D.E. Koppel. 1980. Lateral mobility of integral membrane proteins is increased in spherocyte erythrocytes. *Nature.* 285:510–512.
- Sheetz, M.P., S. Turney, H. Qian, and E.L. Elson. 1989. Nanometre-level analysis demonstrates that lipid flow does not drive membrane glycoprotein movements. *Nature.* 340:284–288.
- Shibamoto, S., M. Hayakawa, K. Takeuchi, T. Hori, K. Miyazawa, N. Kitamura, K.R. Johnson, M.J. Wheelock, N. Matsuyoshi, M. Takeichi, and F. Ito. 1995. Association of p120, a tyrosine kinase substrate, with E-cadherin/catenin complexes. *J. Cell Biol.* 128:949–957.
- Shirayoshi, Y., A. Nose, K. Iwasaki, and M. Takeichi. 1986. N-linked oligosaccharides are not involved in the function of a cell-cell binding glycoprotein E-cadherin. *Cell Struct. Funct.* 11:245–252.
- Takeichi, M. 1988. The cadherins: cell-cell adhesion molecules controlling animal morphogenesis. *Development (Camb.)* 102:639–655.
- Takeichi, M. 1991. Cadherin: cell adhesion receptors as a morphogenetic regulator. *Science.* 251:1451–1455.
- Tsuji, A., and S. Ohnishi. 1986. Restriction of the lateral motion of band 3 in erythrocyte membrane by the cytoskeletal network: dependence on spectrin association state. *Biochemistry.* 25:6133–6139.
- Tsuji, A., K. Kawasaki, S. Ohnishi, H. Merkle, and A. Kusumi. 1988. Regulation of band 3 mobilities in erythrocyte ghost membranes by protein association and cytoskeletal meshwork. *Biochemistry.* 27:7447–7452.
- Wang, Y.-L. 1985. Exchange of actin subunits at the leading edge of living fibroblasts: Possible role of tread milling. *J. Cell Biol.* 101:597–602.
- Wang, Y.-L., J.D. Silverman, and L.-G. Cao. 1994. Single particle tracking of surface receptor movement during cell division. *J. Cell Biol.* 127:963–971.
- Watabe, M., A. Nagafuchi, Sa. Tsukita, and M. Takeichi. 1994. Induction of polarized cell-cell association and retardation of growth by activation of the E-cadherin-catenin adhesion system in a dispersed carcinoma line. *J. Cell Biol.* 127:247–256.